Regional and landscape-scale variability of Landsat-observed vegetation dynamics in northwest Siberian tundra

2014 Environ. Res. Lett. 9 025004

(http://iopscience.iop.org/1748-9326/9/2/025004)

OPEN ACCESS
IOP Publishing
Environmental Research Letters
Environ. Res. Lett. **9** (2014) 025004 (11pp)
doi:10.1088/1748-9326/9/2/025004

Regional and landscape-scale variability of Landsat-observed vegetation dynamics in northwest Siberian tundra

Gerald V Frost[1,3], Howard E Epstein[1] and Donald A Walker[2]

[1] Department of Environmental Sciences, University of Virginia, PO Box 400123, Charlottesville, VA 22903, USA
[2] Alaska Geobotany Center, University of Alaska, PO Box 757000, Fairbanks, AK 99775, USA

E-mail: gvf5y@virginia.edu, jfrost@abrinc.com, hee2b@virginia.edu and dawalker@alaska.edu

Received 6 July 2013, revised 1 November 2013
Accepted for publication 15 January 2014
Published 27 February 2014

Abstract

Widespread increases in Arctic tundra productivity have been documented for decades using coarse-scale satellite observations, but finer-scale observations indicate that changes have been very uneven, with a high degree of landscape- and regional-scale heterogeneity. Here we analyze time-series of the Normalized Difference Vegetation Index (NDVI) observed by Landsat (1984–2012), to assess landscape- and regional-scale variability of tundra vegetation dynamics in the northwest Siberian Low Arctic, a little-studied region with varied soils, landscape histories, and permafrost attributes. We also estimate spatio-temporal rates of land-cover change associated with expansion of tall alder (*Alnus*) shrublands, by integrating Landsat time-series with very-high-resolution imagery dating to the mid-1960s. We compiled Landsat time-series for eleven widely-distributed landscapes, and performed linear regression of NDVI values on a per-pixel basis. We found positive net NDVI trends ('greening') in nine of eleven landscapes. Net greening occurred in alder shrublands in all landscapes, and strong greening tended to correspond to shrublands that developed since the 1960s. Much of the spatial variability of greening within landscapes was linked to landscape physiography and permafrost attributes, while between-landscape variability largely corresponded to differences in surficial geology. We conclude that continued increases in tundra productivity in the region are likely in upland tundra landscapes with fine-textured, cryoturbated soils; these areas currently tend to support discontinuous vegetation cover, but are highly susceptible to rapid increases in vegetation cover, as well as land-cover changes associated with the development of tall shrublands.

Keywords: tundra, vegetation dynamics, Landsat, normalized difference vegetation index (NDVI), shrub expansion, permafrost, climate change, Siberia

S Online supplementary data available from stacks.iop.org/ERL/9/025004/mmedia

1. Introduction

Rapid changes in climate are driving a suite of changes to the physical and biological properties of Arctic terrestrial and marine ecosystems. The dramatic reduction in the extent of summer sea-ice in recent decades has garnered the most attention, and is a key driver of a phenomenon known as 'Arctic amplification', by which climate-induced changes to the Arctic land- and sea surface create positive feedbacks that promote

[3] Author to whom any correspondence should be addressed. Present address: ABR, Inc. Environmental Research and Services, PO Box 80410, Fairbanks, AK 99708, USA.

further warming (Serreze and Barry 2011). Changes to the structure of tundra vegetation, such as increasing height and extent of erect, canopy-forming shrubs, are also dynamically linked with the climate system (Chapin *et al* 2005), and affect a wide range of processes in Arctic landscapes including biogeochemical cycling, hydrology, permafrost dynamics, and land-use by wildlife and humans (Hinzman *et al* 2005, Forbes *et al* 2009, Myers-Smith *et al* 2011). Changes to tundra vegetation are relatively difficult to assess, however, as most tundra plant communities are dominated by long-lived, slow-growing species and observable changes generally require decades.

Widespread increases in remotely-sensed measures of vegetation productivity, primarily the Normalized Difference Vegetation Index (NDVI), have been observed at high latitudes using Advanced Very High Resolution Radiometer (AVHRR) datasets obtained since 1981 (Myneni *et al* 1997, Jia *et al* 2003, Bhatt *et al* 2010), a phenomenon frequently termed the 'greening of the Arctic'. AVHRR provides a daily, global dataset with a long period-of-record (1981-present), thus making it well-suited for circumpolar-scale trend detection. At the $\sim$8 km spatial resolution of global AVHRR datasets, however, landscape-scale changes to vegetation and land-cover are rendered as 'sub-pixel' effects. Field-based and remote-sensing observations at finer scales indicate that recent vegetation dynamics have been very uneven, with a high degree of heterogeneity evident at regional- and landscape scales (McManus *et al* 2012, Tape *et al* 2012, Raynolds *et al* 2013). Circumpolar greening therefore describes a general pattern of increasing tundra productivity, but other techniques are necessary to determine specific changes to vegetation and their underlying, biophysical causes. Bridging this gap is a critical component of efforts to understand how tundra vegetation is changing in space and time, the concomitant impacts to landscape processes, and to improve projections of future environmental change.

Several recent studies have applied 30 m resolution multi-spectral Thematic Mapper (TM) and Enhanced Thematic Mapper (ETM+) data from the Landsat family of satellites, to investigate tundra vegetation dynamics in Canada (Fraser *et al* 2011, McManus *et al* 2012) and Alaska (Raynolds *et al* 2013). Landsat data offer an intermediate spatial scale that is adequate to isolate spectral trends within landscape components of interest, such as individual vegetation types, geomorphic landforms, and human-affected areas. Landsat data are well-suited for time-series analysis, because the data are well-calibrated over time, and robust methods have been developed to correct for atmospheric conditions at the time of image acquisition (e.g., the Landsat Ecosystem Disturbance Adaptive Processing System [LEDAPS] (Masek *et al* 2006)). Additionally, the observational period of Landsat TM/ETM+ data (1984-present) is similar to AVHRR, facilitating greater integration and contextualization of information obtained from the field-scale (meters) to the circumpolar scale.

The northwest Siberian Arctic, here defined as the area extending from the Polar Ural Mountains eastward to the Taymyr Peninsula, is a geographically large region which has experienced pronounced environmental, societal, and land-use changes in recent decades (Stammler 2005, Walker *et al* 2009a, Forbes *et al* 2009, 2010). AVHRR observations indicate a great deal of heterogeneity in NDVI trends in the region, with spatially-contiguous zones of both greening and browning evident (Bhatt *et al* 2010). One possible explanation for this spatial variability, is that the wide variation in surficial geology, soils, and permafrost attributes in the region (Leibman 1995, Drozdov *et al* 2005, Walker *et al* 2009a, 2012) strongly modulates the local responses of vegetation to recent climatic changes. Northwest Siberian tundra has received comparatively little study, but available information highlights increases in the productivity and extent of tundra shrubs as a key driver of regional greening patterns (Forbes *et al* 2010, Walker *et al* 2012, Macias-Fauria *et al* 2012, Frost *et al* 2013), as has been reported elsewhere in the Arctic (Myers-Smith *et al* 2011).

Figure 1. Ground photo of recently-established alders in Kharp study landscape.

In this paper, we apply time-series of Landsat NDVI to assess landscape- and regional-scale variability of tundra vegetation dynamics across a series of Low Arctic landscapes spanning northwest Siberia. We also focus on an important form of land-cover change in the region, the proliferation of tall shrublands (>2 m height) dominated by Siberian alder (*Alnus viridis* ssp. *fruticosa*), the establishment of which represents a fundamental change to tundra vegetation structure (figure 1). Our specific objectives were to (1) map statistically-significant trends of Landsat NDVI across eleven widely-distributed tundra landscapes, and relate the spatial variability of trends to local and regional attributes of landscape physiography, soils, permafrost, and disturbance regime; (2) isolate the spectral trends of newly-established tall shrubland patches, by applying results from a previous study (Frost and Epstein 2014) that quantified changes in shrubland cover at five of the landscapes using very-high-resolution (VHR; <2 m pixel^{-1}) imagery from 1966–1968 and 2005–2011; and (3) develop empirical functions to estimate rates of recent shrub expansion in six, much larger landscapes based on the spectral trends of shrublands.

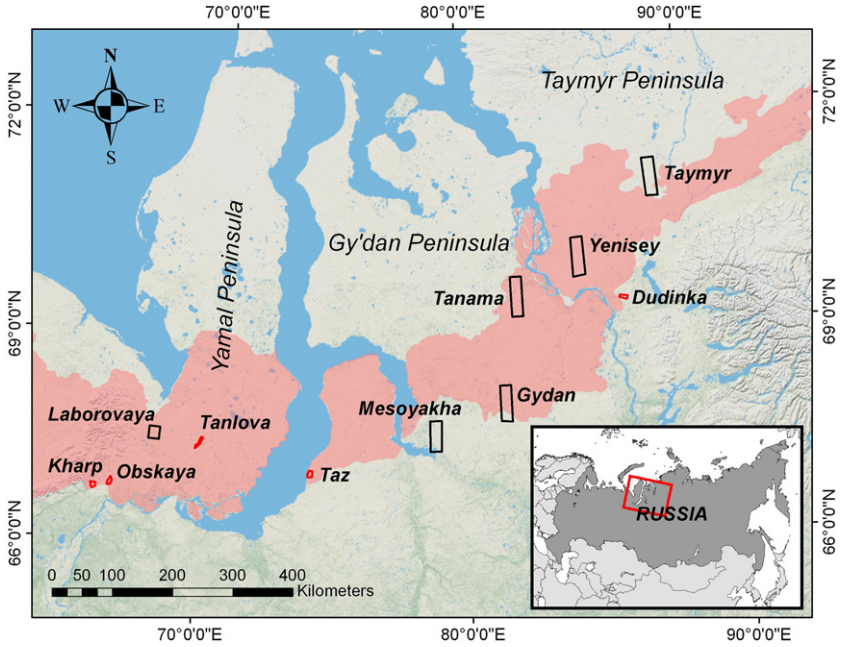

Figure 2. Locations of the study landscapes in northwest Siberia; the shaded area represents bioclimate subzone E (CAVM Team 2003). Intensive landscapes used to associate shrub expansion areas with Landsat NDVI trends are outlined in red; regional landscapes are outlined in black.

2. Methods

2.1. Data sources and study areas

We examined spectral trends observed by Landsat within eleven tundra-dominated study areas spanning northwest Siberia (figure 2). The eleven study areas consist of (1) five *intensive* study landscapes (~ 65 km^2) for which shrub-driven changes in land-cover are known from comparisons of declassified 'Corona' and 'Gambit' VHR imagery from the mid-1960s, and recent VHR imagery (2005–2011) (see Frost and Epstein 2014); and (2) six much larger *regional* study landscapes (~500–1,200 km^2) that lack 1960s imagery. Landsat data for northwest Siberia come from 1984–1988 and 1999–2012; Landsat data acquisition was suspended for most Arctic regions during 1989–1998, therefore we only analyzed landscapes for which at least two observations exist for the mid-1980s. We restricted analyses to imagery acquired during a 30-day period in mid- to late summer (22 July to 21 August), when live phytomass and NDVI are at their seasonal peak (hereafter, 'peak NDVI'). To maximize the number of time-steps available for analysis, we accepted some scenes with partial cloud cover; for such scenes, we manually masked clouds and cloud shadows. We also used scenes acquired by Landsat 7 after 2003, which contain 'scan-line' data gaps. We converted the top-of-atmosphere radiance values in the raw imagery to surface reflectance using the LEDAPS algorithm (Masek *et al* 2006). We then calculated the NDVI for each pixel using the surface reflectance values in the near-infrared and red bands (Tucker and Sellers 1986). To evaluate potential bias in the timing of peak NDVI within this 30-day window, we determined the correlation between observed NDVI and the Julian day of imagery acquisition; we found no correlation for any landscape ($r^2 \leq 0.12$; $p \geq 0.3$) (supplementary figure S1 available at stacks.iop.org/ERL/9/025004/mmedia).

We identified study landscapes by examining modern VHR imagery archives for bioclimate subzone 'E' of the Circumpolar Arctic Vegetation Map (Walker *et al* 2005); this subzone refers to the warmest, southernmost part of the Arctic tundra biome, where the proliferation of tall shrubs is an important land-cover change issue (Myers-Smith *et al* 2011). Imagery coverage is sparse in northwest Siberia, so we made opportunistic use of cloud-free, summer imagery acquired by five commercial satellites (table 1). Most of the study landscapes lie entirely within bioclimate Subzone E; those that do not are dominated nonetheless by tundra vegetation typical of this subzone (i.e., little or no tree cover, but tall shrublands are common). All landscapes primarily encompass gently-sloping, upland terrain dissected by small alluvial valleys. Some landscapes also encompass well-developed river floodplains; more detailed descriptions of the five intensive study landscapes can be found in Frost and Epstein (2014) and Frost *et al* (2013). Instrumental records for 1965–2010 from six meteorological stations in the region indicate mean annual temperatures of −11.4 to −6.1°C, mean growing-season temperatures (June–August) of 8.7–11.5 °C, and mean annual precipitation of 293–515 mm (monthly means acquired from the National Climatic Data Center www.ncdc.gov). All of these stations recorded significant warming trends in growing-season temperature ($p < 0.05$) since the mid-1960s (i.e., the period-of-record for VHR imagery at the intensive study landscapes); however, since the early 1980s there has been high inter-annual variability and no trend is evident in growing-season temperature.

Table 1. Summary of locations, historical and modern VHR imagery attributes, and Landsat TM/ETM+ period-of-record for the study landscapes.

Landscape	Latitude (°N)	Longitude (°E)	Area (km^2)	Historical VHR imagery[a]	Modern VHR imagery[b]	Landsat period-of-record
Kharp	66.8	66.0	66	19/8/1968 (KH-4B)	21/6/ 2010 (WV-1)	1985–2010
Obskaya	66.9	66.6	62	19/8/1968 (KH-4B)	3/6/2011 (WV-2)	1984–2010
Laborovaya	67.7	68.1	364	—	11/7/2005 (QB-2)	1984–2012
Tanlova	67.6	69.8	69	21/8/1968 (KH-4B)	22/7/2011 (WV-2)	1986–2011
Taz	67.2	74.0	75	21/8/1968 (KH-4B)	20/8/2010 (WV-1)	1987–2012
Mesoyakha	67.8	78.82	964	—	2/9/2005 (QB-2)	1985–2011
Gydan	68.2	81.6	1080	—	9/7/2009 (GE-1)	1985–2011
Tanama	69.7	82.2	1223	—	23/8/2009 (QB-2)	1985–2012
Yenisey	70.2	84.8	1259	—	6/7/2010 (GE-1)	1985–2010
Dudinka	69.6	86.5	65	15/7/1966 (KH-7)	9/7/2009 (GE-1)	1985–2012
Taymyr	71.2	88.2	1226	—	9/7/2010 (GE-1)	1985–2012

[a] KH-4B = Corona, KH-7 = Gambit.
[b] WV-1 = WorldView-1, WV-2 = WorldView-2, QB-2 = QuickBird, GE-1 = GeoEye-1.

Table 2. Physiographic units used to stratify the study landscapes.

Physiographic unit	Description
Upland	Slopes and plateaus with high position in local topography
Lowland	Moisture-gathering, non-floodplain areas occupying low position in local topography, flat or with low relief ($\leq 1°$ slope)
Riverine	Active floodplains and adjacent landforms formed by fluvial processes
Waterbody	Perennial lakes, ponds, and river channels

2.2. Imagery analysis

At the five intensive study landscapes, we quantified changes in alder shrubland cover since the 1960s by comparing 1960s VHR imagery with imagery from recent years (see Frost and Epstein (2014) for detailed methods). Briefly, we co-registered the 1960s imagery with the modern VHR ortho-images, and overlaid a uniform grid of sampling-points at 30 m spacing, so as to match the spatial resolution of Landsat imagery. We then visually recorded the presence/absence of alder shrub cover at each sampling-point for 1960s and modern imagery, and assigned this value to the corresponding Landsat pixel; grids were oriented such that sampling-points were at the center of each Landsat pixel.

For the six regional study landscapes, we delineated present-day alder shrublands using modern multi-spectral VHR imagery. The tall stature, high biomass, dark foliage, and extensive intra-canopy shadowing of alder shrublands produce distinct spectral signatures within otherwise low-growing tundra vegetation. We used the Interactive Supervised Classification tool in ArcMap v. 10.1 (ESRI; Redlands, CA) to delineate alder shrublands, based on the spectral attributes of small 'training' polygons that we manually digitized in representative shrubland patches. Other shrubs, such as dwarf birch (*Betula nana*) and willows (*Salix*), are also common in the study region, but are generally low-growing; however, they were sometimes confused with tall alder shrublands (e.g., on floodplains). We therefore visually identified, and manually corrected errors in the classification. We used similar techniques to delineate lakes and other waterbodies, which we excluded from subsequent NDVI time-series analysis. Finally, we generated a grid of sampling-points as described for the intensive study landscapes, and assigned the corresponding land-cover class (tall alder, tundra, or water) and Landsat NDVI pixel stack to each sampling-point.

At all landscapes, we performed least-squares linear regression for each pixel stack, with year as the independent variable and NDVI as the response variable. We then calculated the slope of the trendline (the annual rate of 'greening' or 'browning') for stacks with significant trends ($p \leq 0.05$). At the five intensive study landscapes, we used the vegetation sampling-grid data to stratify pixel stacks according to three land-cover classes: (1) newly-established shrubland (i.e., did not exist in the 1960s); (2) pre-existing shrubland (i.e., already present in the 1960s); and (3) low-growing tundra. At the six regional study landscapes, we distinguished present-day alder shrublands as a single class (because the 1960s shrubland extent was unknown), and a tundra land-cover class.

We applied digital elevation models (DEMs) and VHR imagery to delineate four physiographic divisions within each landscape: upland, lowland, riverine, and waterbody (table 2). These physiographic divisions integrate environmental state factors related to soils, moisture regime, disturbance regime, and landscape-forming processes. DEMs were derived from Russian topographic maps and have a nominal horizontal resolution of ~ 70 m. We first orthorectified all modern VHR imagery in ArcMap using the imagery metadata and the DEMs. To delineate the lowland physiographic unit, we used the 'flow accumulation' tool in ArcMap to classify DEM grid cells that received hydrologic inputs from ≥ 200 upslope cells.

Table 3. Summary of Landsat NDVI trends at the study landscapes for alder shrublands and tundra.

		% of landscape greening			% of landscape browning		
Landscape	Mean *n* of Landsat observations	Total	Alder	Tundra	Total	Alder	Tundra
Kharp	11.6	61.9	81.8	59.1	0.1	0	0.1
Obskaya	10.8	58.5	70.4	57.2	0	0	0
Laborovaya	11.9	10.9	18.2	10.8	0.8	0	0.8
Tanlova	9.7	6.2	19.4	5.0	10.6	4.6	11.2
Taz	8.8	4.8	4.6	4.9	0.2	0	0.2
Mesoyakha	11.1	3.3	15.4	3.2	5.7	0.7	5.7
Gydan	8.9	22.4	54.6	21.5	0.3	0	0.3
Tanama	8.6	23.4	58.4	22.4	0.2	0	0.2
Yenisey	10.2	28.9	27.4	28.9	0.2	0.1	0.2
Dudinka	12.4	63.9	53.1	68.7	0	0	0
Taymyr	9.2	9.7	54.6	9.6	0.3	0	0.3

This step identified drainage corridors, ranging in size from small, first-order streams, to large rivers. We then classified as lowland, all DEM grid cells that had a slope angle of $\leq 1°$, and were linked to drainages by a spatially continuous field of other flat cells. The upland physiographic unit included all areas with a slope angle $>1°$, and flat grid cells that were not linked to drainages (i.e., upland plateaus). We manually digitized the riverine physiographic unit through photo-interpretation of characteristic riverine landforms (e.g., point bars, cutbanks, oxbows) in modern VHR imagery. We then stratified all Landsat pixel stacks by physiographic unit.

We estimated the rate of recent alder shrubland expansion in the six regional study landscapes, based on patterns of variation in NDVI trends observed in newly-established and pre-existing shrublands at the five intensive landscapes. We first calculated frequency distributions of rates of greening for pixel stacks with significant trends ($p < 0.05$) in newly-established, and pre-existing alder shrublands in the intensive landscapes; we hereafter refer to these frequency distributions as 'NDVI response curves'. To generate NDVI response curves, we binned all significant NDVI trend observations into small increments (.005 NDVI units decade^{-1}), and plotted the percentage of all pixels in each shrubland class (regardless of significance) that belonged to each bin. We also calculated the integral of each NDVI response curve, to determine the percentage of pixels in each shrubland class that had significant NDVI trends.

To estimate rates of alder expansion within the six regional study landscapes, we used the NDVI response curves to determine the probability that a given shrubland pixel corresponded to newly-established alder cover, based on its rate of greening. We multiplied the number of shrubland pixels within each bin of NDVI trend, by a coefficient representing the proportion of alder pixels for that bin that belonged to the newly-established shrubland class at the intensive study landscapes. We then summed the number of pixels assigned to newly-established shrubland for each bin, according to the equation

$$\sum_{i=1}^{n} = p_i(x_i)$$

where $n =$ the total number of bins of NDVI trend, p is the probability that a pixel in bin n corresponded to newly-established shrub cover, and x is the total number of pixels for that bin. We calculated the extent of new shrubs on a percent basis, by normalizing the number of newly-established shrubland pixels against the number of pre-existing shrubland pixels. We then converted this value to a decadal expansion rate (% shrub increase decade^{-1}), based on the period-of-record for VHR observations (42 or 43 years). We evaluated the accuracy of this approach, by estimating the spatial extent of shrub expansion at each intensive landscape independently using NDVI response curves generated from the other four intensive landscapes.

3. Results

3.1. Landscape-wide NDVI trends

We observed net greening at nine landscapes, and net browning at two landscapes (table 3). Among the nine landscapes in which net greening occurred, the proportion of Landsat pixel stacks with significant, positive trends varied widely (4.8–63.9%; median 23.4%), but very few stacks had negative trends (0–0.8%; median 0.2%). Among the two landscapes in which net browning occurred, the proportion of pixel stacks with negative trends was comparatively small (5.7 and 10.6%), and greening occurred in some areas (3.3 and 6.2%).

Within each landscape, the net direction of NDVI trends was the same for all physiographic units, but the extent of greening was disproportionately high in uplands at several landscapes (figure 3). Among the nine landscapes in which net greening occurred, the percentage of pixels with greening trends was highest for uplands in five landscapes (5.7–65.1%; median 42.2%), for lowlands in two landscapes (5.4 and 29.2%), and for riparian areas in two landscapes (44.4 and 61.1%). The spatial extent of uplands was much greater than that of other physiographic units in seven of these landscapes, however, and greening in uplands accounted for most of the total greening in eight landscapes. At Laborovaya and Yenisey, the proportion of greening pixel stacks was highest in lowlands, but we observed a similar proportion

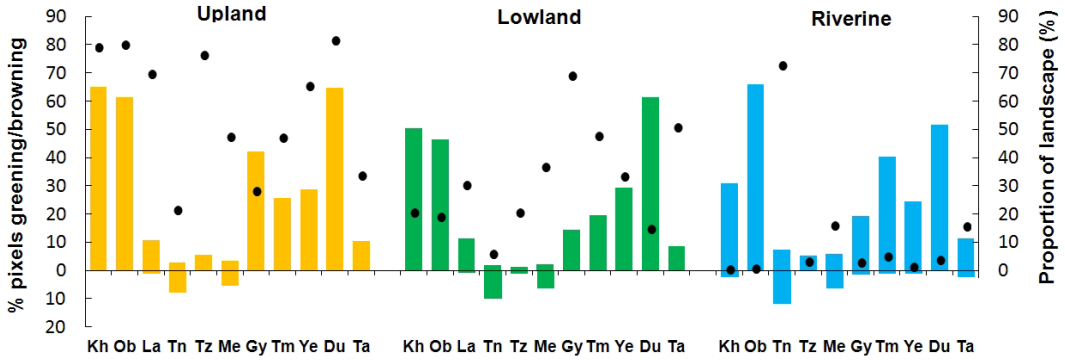

Figure 3. Proportion of Landsat pixel stacks with significant NDVI trends by physiographic unit (colored bars, plotted on left axis), and the proportion of each landscape comprised by each physiographic unit (black markers, right axis). Values above the x-axis indicate greening; values below the x-axis indicate browning.

of greening pixels in upland stacks; additionally, much of the lowland greening at Laborovaya occurred along a railway corridor disturbed by construction activities beginning in the 1980s. Trends varied the most in riverine areas; although we observed widespread greening in riverine areas in several landscapes, the extent of riparian areas was very limited in most landscapes, and net browning occurred in the two landscapes with extensive floodplains (Tanlova and Mesoyakha).

3.2. Shrubland spectral trends

Net greening occurred in alder shrublands at all eleven study landscapes (4.6–81.8%; median 53.1%), including two landscapes in which browning was widespread in tundra communities (table 3). We observed virtually no browning in alder shrublands except at two landscapes (Tanlova and Mesoyakha; 0.7 and 2.5% of shrubland pixels respectively). The proportion of present-day alder shrubland pixels with greening trends was greater than the proportion of tundra pixels with greening trends at eight landscapes, but was slightly lower at three landscapes.

At the five intensive study landscapes, we categorized alder shrublands as newly-established and pre-existing, using comparisons of VHR imagery from the 1960s and recent years. Shrubland cover increased +1.3–6.0% decade^{-1} in these landscapes (Frost and Epstein 2014), and Landsat pixel stacks with strong greening trends tended to coincide with known shrub expansion areas (figure 4). Across all five intensive landscapes, 70.3% of Landsat pixel stacks in newly-established shrublands had significant greening trends, and the mean rate of greening was 0.047 NDVI units decade^{-1} (landscape mean range 0.040–0.051). In pre-existing shrublands, 42.3% of Landsat pixels had significant greening trends, and the mean rate of greening was 0.035 units decade^{-1} (landscape mean range 0.023–0.041). NDVI response curves indicate that low rates of greening (<0.03 NDVI units decade^{-1}) occurred in similar proportions of Landsat pixels in pre-existing and newly-established shrublands; however, shrublands with greening trends ≥0.045 units decade^{-1} were at least twice as likely to correspond to newly-established shrublands (figure 5(a)). Rates of recent (post-1965) shrub expansion estimated from NDVI response curves for the eleven study landscapes range from +0.4–5.7% decade^{-1} (table 4). Although the magnitude of these estimates are comparable to the range observed for the five intensive landscapes using VHR imagery comparisons, independent accuracy assessments generally indicate poor agreement between shrub expansion rates estimated from Landsat data, and rates observed at the intensive sites, particularly for the Kharp landscape (figure 5(b)).

Table 4. Decadal rate of change in alder shrubland extent estimated from Landsat NDVI trends for all landscapes, and observed from comparisons of VHR imagery from the 1960s and recent years for the five intensive study landscapes.

Landscape	Modern shrub cover (ha)	Estimated shrub expansion rate (%Δ decade^{-1})	Observed shrub expansion rate (%Δ decade^{-1})
Kharp	773	5.2	2.0
Obskaya	585	5.7	4.8
Laborovaya	260	0.8	—
Tanlova	395	2.4	4.5
Taz	1277	0.4	1.3
Mesoyakha	1116	0.7	—
Gydan	2652	3.7	—
Tanama	3207	2.8	—
Yenisey	1624	1.3	—
Dudinka	1617	3.9	6.0
Taymyr	128	3.2	—

4. Discussion

4.1. Landscape-wide NDVI trends

We observed greening in all three physiographic units at eight landscapes distributed in the foothills of the Polar Ural Mountains, and the Gydan and Taymyr Peninsulas; however, greening was generally most widespread in upland areas (figure 6). The prevalence of greening that we observed in upland terrain is somewhat inconsistent with other landscape-scale studies that have applied Landsat NDVI time-series elsewhere in the Arctic. For example, greening observed in

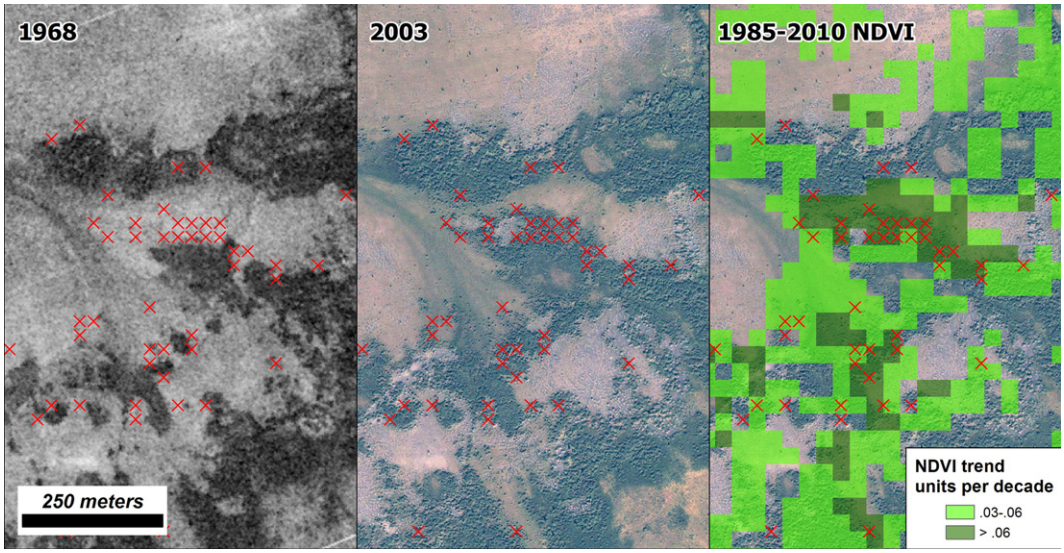

Figure 4. Corona (left) and QuickBird (center) imagery for part of the Kharp landscape. Alder shrublands (dark patches) contrast sharply with tundra; red markers indicate Landsat pixel stacks with newly-established shrub cover. Landsat time-series for 1985–2010 (right) show disproportionately high greening in shrublands; pixels with non-significant trends ($p > 0.05$) are not shown.

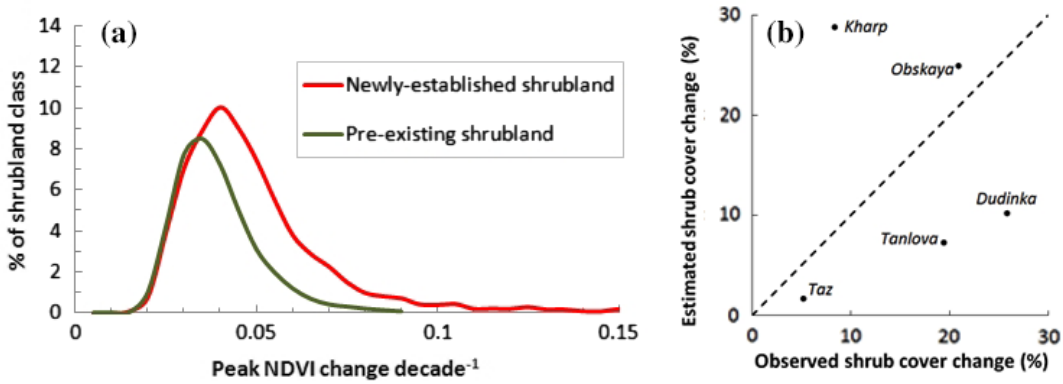

Figure 5. (a) NDVI response curves for pixel stacks in pre-existing and newly-established shrublands identified in 1960s and modern VHR imagery at the five intensive landscapes. Curves are plotted as a percentage of all pixel stacks for the two categories. (b) Accuracy assessment of Landsat estimates of the spatial extent of newly-established shrublands, and the extent observed in VHR imagery comparisons for the intensive study landscapes. Estimates were computed independently for each intensive landscape, using NDVI response curves generated from the other four intensive landscapes.

the Canadian Arctic by Fraser *et al* (2011) was primarily concentrated in valley bottoms and other low-lying areas, and McManus *et al* (2012) observed similar landscape-scale patterns of NDVI trend in Low Arctic Quebec. These apparent inconsistencies highlight that although spatial patterns of tundra greening can be generalized to some degree at landscape- and even regional scales, unifying explanations for spatial patterns of greening and their causal mechanisms at the circumpolar scale remain elusive. Widespread warming observed across most of the circumpolar Arctic during the 20th century plausibly explain the positive trends evident in coarse-scale datasets, such as AVHRR, but findings derived from fine-scale datasets indicate that other environmental factors, such as differences in substrates, geomorphic processes, and disturbance regime, likely promote a high degree of variability in the susceptibility of Arctic landscapes to environmental change.

Net trends of NDVI were positive at most of the landscapes that we studied, but we did observe browning in two landscapes (Tanlova and Mesoyakha), and little net trend in a third landscape (Taz) (figure 3). These three landscapes are located on the southern Yamal and Tazovskiy peninsulas, which share similar surficial geology dominated by sandy marine sediments (Drozdov *et al* 2005). Walker *et al* (2009a) noted a close correspondence between low-productivity tundra communities and sandy uplands on the Yamal; soils in these areas are relatively old and tend to be highly leached, with low concentrations of nitrogen and cations (Walker *et al* 2009b). Modern VHR imagery indicates that uplands at Tanlova and Mesoyakha have not been extensively disturbed by cryogenic landslides and other erosional processes, which expose underlying marine clays with much higher nutrient content (Leibman 1995, Walker *et al* 2009a). Comparison of 1960s

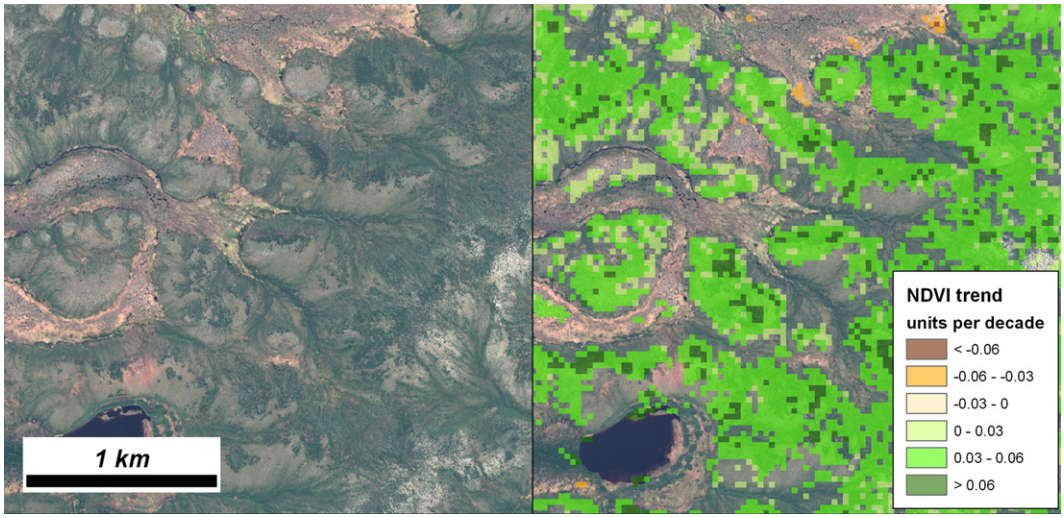

Figure 6. Upland and lowland terrain at Gydan landscape (GeoEye; left), and overlay of significant trends of Landsat NDVI (1985–2011; right). In the GeoEye image, lowland vegetation is yellowish, upland tundra is grayish-green, and darkest green patches correspond to alder shrublands. Little greening occurred in lowland tundra, and the strongest greening is coincident with shrubby areas.

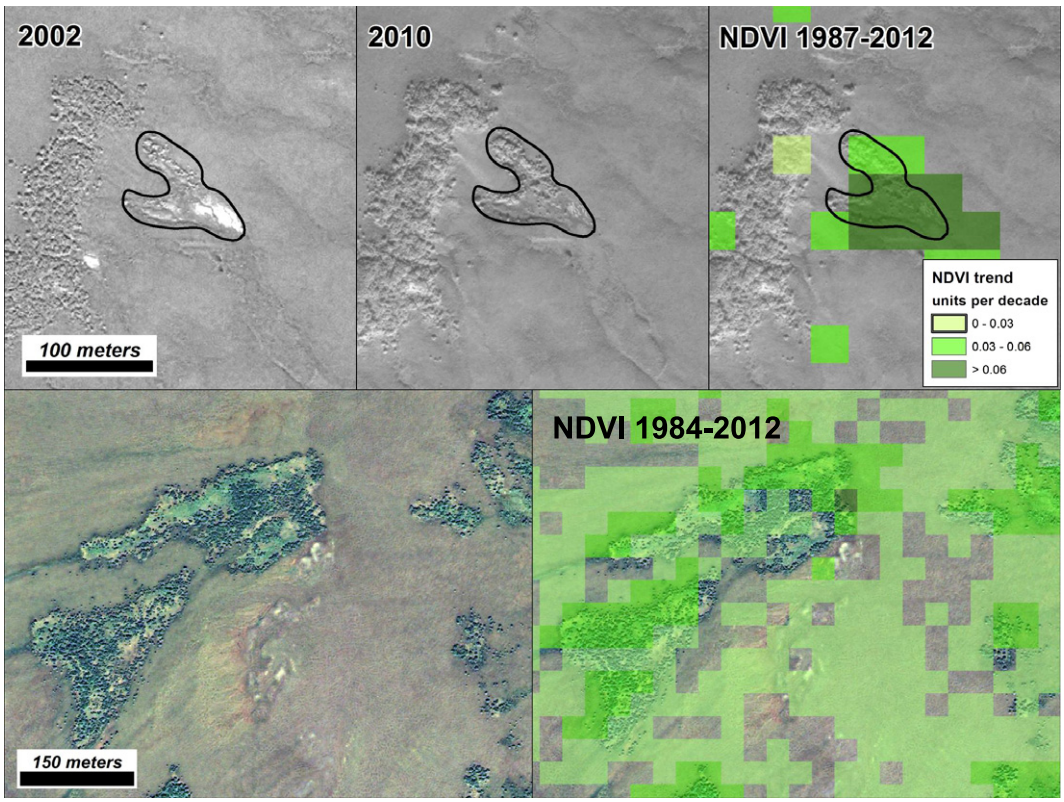

Figure 7. (a) Cryogenic landslide (black outline) at Taz shown in 2002 (IKONOS; upper left), and 2010 (WorldView-1; upper center), and significant NDVI trends (upper right). Note the rapid development of alder shrubs after only 8 year. (b) Patterned-ground area at Laborovaya; note the reticulated photo-signature of non-sorted circles in tundra (QuickBird; lower left); widespread greening occurred in patterned-ground and especially in alder shrublands (lower right).

and modern VHR imagery at Tanlova indicates that although alder shrubland extent increased markedly, virtually all of the increase occurred on floodplains and there was virtually no change in sandy, undisturbed uplands. Sandy uplands are also extensive at Taz, but erosional features are more widespread and shrub expansion occurred locally on hillslopes affected by cryogenic landslides (figure 7(a)), a pattern consistent with the distribution of highly-productive willow shrublands on landslides farther north on the Yamal (Leibman 1995, Ermokhina and Myalo 2012).

Contrasts in the relative extent of greening between the Yamal and Tazovskiy peninsulas, and the rest of the study region are striking considering that multi-decadal climate trends and variability have been similar over the entire study domain. One explanation for these regional-scale differences in vegetation dynamics, is that differences in surficial geology and landscape-forming processes result in large contrasts in edaphic conditions and disturbance regime, which promote the development of dissimilar tundra communities on sandy and fine-textured substrates (see Walker *et al* 2012). These communities, in turn, can be expected to exhibit different responses to shared climatic trends in recent decades. In contrast to the sandy marine sediments of the Yamal and Tazovskiy regions, soils at the Ural foothills landscapes are derived from mafic bedrock, while clayey marine and fluvio-glacial deposits are widespread in the Gydan and Taymyr Peninsula regions (Drozdov *et al* 2005). These parent materials promote the formation of fine-textured soils, which have markedly different hydrologic and chemical properties compared to sandy substrates. Additionally, fine-textured soils are more subject to cryoturbation related to seasonal frost heave (Peterson and Krantz 2003, Walker *et al* 2004). Examination of VHR imagery, and field studies at two landscapes (Kharp and Obskaya; see Frost *et al* (2013)), indicate that much of the upland greening in the Urals, Gydan, and Taymyr regions is strongly linked to cryogenic disturbance processes in areas of patterned-ground with abundant, sorted- and non-sorted circles (figure 7(b)). Although it is difficult to quantify the extent of circles over large areas due to the small size of individual features, patterned-ground mosaics are widespread in upland terrain in much of the northwest Siberian Arctic, particularly in landscapes dominated by fine-textured mineral soils that are highly susceptible to cryoturbation (supplemental figure S2 available at stacks.iop.org/ERL/9/025004/mmedia). These areas tend to support discontinuous vegetation cover, because strong cryogenic disturbance at circles inhibits the establishment of vegetation. In warmer parts of the Arctic, however, these microsites can be rapidly colonized by vegetation, where the encroachment of relatively fast-growing species can attenuate cryoturbation and promote the development of continuous vegetation cover (Walker *et al* 2008, Shur *et al* 2009).

4.2. Alder shrubland spectral trends

In the five intensive study landscapes, we observed disproportionately strong greening trends in alder shrublands that were known to have become established since the 1960s, but we also observed extensive greening in pre-existing shrublands. The overlap in NDVI trends observed in shrublands of varying age, and variability in the degree of this overlap across the five intensive landscapes, introduced considerable error in the empirical functions used to estimate shrub expansion rates based on NDVI trend (table 4; figure 5). Our findings indicate that although spatio-temporal trends of Landsat NDVI are qualitatively consistent with patterns of shrub expansion, and are effective at identifying 'hotspots' of change, the use of Landsat time-series to produce quantitative estimates of landscape-wide shrub expansion rates remains a challenge. We suggest, however, that future efforts to model rates of tundra shrub increase at the landscape scale using Landsat data, may benefit by improving on some of the shortcomings of the methods and available data applied here. We classified newly-established, and pre-existing shrublands using a point-intercept sampling approach, such that changes in the cover or density of shrubs elsewhere within a 900 m^2 Landsat pixel were not accounted for. This mismatch in sampling of points, versus pixels undoubtedly introduced confusion between pre-existing and newly-established shrubland classes. Additionally, increases in alder shrubland extent are likely to often occur against a backdrop of 'background greening' associated with more subtle changes within the matrix of tundra vegetation surrounding the shrub patches. Finally, the sensitivity of Landsat NDVI observations to incremental increases in biomass is substantially reduced where high biomass is already present (figure 8), a relationship that has also been noted in AVHRR data (Raynolds *et al* 2012). Therefore, while the development of alder shrublands on sparsely-vegetated sites can be expected to produce strong positive NDVI trends, increases in shrub density within high-biomass stands likely have a small influence on Landsat-observed NDVI; error introduced by this diminished sensitivity were probably exacerbated by the fact that some of the shrub expansion observed at the five intensive landscapes had occurred before the Landsat TM/ETM+ era began.

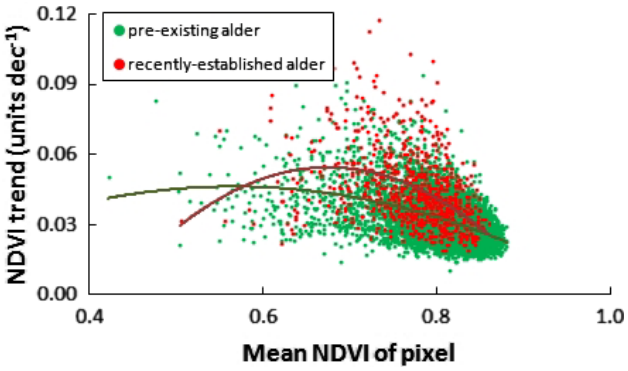

Figure 8. Scatterplot of mean NDVI, versus mean NDVI trend for pre-existing, and newly-established shrublands at Kharp. Note the diminishing magnitude of NDVI trends at increasing values of NDVI.

The widespread, and disproportionate positive trends in NDVI that we observed in alder shrublands throughout the study area are broadly consistent with increased shrubland extent and productivity, regardless of the timing of shrub establishment. Although the overall extent of alder shrublands is low in several of the study landscapes, the ubiquity of greening in high-biomass shrublands—even at the northern margin of alder's distribution at the coldest, Taymyr landscape—indicates that tall shrubland development is occurring at a wide scale in the northwest Siberian Low Arctic, and there appears to be high potential for further increase. The facilitation of alder recruitment on meter-scale patterned-ground features has been described in detail from field studies at the Kharp and Obskaya landscapes (see Frost *et al* (2013)) and plausibly

explains the widespread greening seen in alder shrublands at most of the other landscapes. Broader patterns of greening indicate, however, that alder shrubland development is likely only one, conspicuous part of a broader pattern of vegetation development in active patterned-ground areas of the region.

4.3. Agreement with other NDVI time-series

One limitation of Landsat-based analyses of tundra vegetation dynamics is the lack of data for 1989–1998 for much of the Arctic, raising the possibility that the linear NDVI trends reported here might mask non-linear dynamics that would have been apparent were data available for this 'lost decade'. One way to address this issue is to compare our findings with those from studies that applied similar techniques to AVHRR time-series, which provide a continuous record since 1981. The three landscapes in which we observed flat, or negative Landsat NDVI trends correspond with areas of little or no trend in AVHRR time-series (Bhatt *et al* 2010); additionally, the widespread greening that we observed in the Gydan and Taymyr Peninsula regions is corroborated by AVHRR. The strong greening we report for three intensive study landscapes in the Ural foothills and southwestern Taymyr, however, is not evident in AVHRR time-series. This inconsistency is likely attributable in part to a mismatch in the spatial resolution of the two datasets; these three landscapes represent areas of only ~60 km^2, and therefore encompass small portions of several adjacent AVHRR pixels. Nonetheless, this lack of agreement warrants further investigation, because the Landsat-observed greening in these areas is corroborated by historical and modern VHR imagery, which indicates widespread increases in the extent of high-biomass shrublands.

Acknowledgments

This work was funded by the NASA Land-Cover Land-Use Change Initiative (LCLUC), grants NNG6GE00A and NNX09AK56G; the Virginia Space Grant Consortium (VSGC); and the Department of Environmental Sciences at the University of Virginia. We also thank the National Geospatial-Intelligence Agency Commercial Imagery Program for permitting access to NGA satellite imagery archives; we especially thank Jaime Nickeson at NASA and Paul Morin at the University of Minnesota for delivering useful data. Useful DEMs for the study area came from the European Space Agency's DUE Permafrost Project. Finally, we thank Kathy Holcomb at the University of Virginia for automating processing steps for Landsat data.

References

Bhatt U S *et al* 2010 Circumpolar arctic tundra vegetation change is linked to sea ice decline *Earth Interact* **14** 1–20

CAVM Team 2003 *Circumpolar Arctic Vegetation Map* (1:7,500,000 scale). Conservation of Arctic Flora and Fauna (CAFF) Map No. 1 (Anchorage, AK: US Fish & Wildlife Service)

Chapin F S III *et al* 2005 Role of land-surface changes in Arctic summer warming *Science* **310** 657–60

Drozdov D S, Rivkin F M, Rachold V, Ananjeva-Malkova G V, Ivanova N V, Chehina I V, Koreisha M M, Korostelev Y V and Melnikov E S 2005 Electronic atlas of the Russian Arctic coastal zone *Geo-Mar. Lett.* **25** 81–8

Epstein H E, Raynolds M K, Walker D A, Bhatt U S, Tucker C J and Pinzon J E 2012 Dynamics of aboveground phytomass of the circumpolar Arctic tundra during the past three decades *Environ. Res. Lett.* **7** 015506

Ermokhina K A and Myalo E G 2012 Phytoindicators of landslide disturbances in the central yamal *Proc. 10th International Conf. on Permafrost.* vol 2, pp 531–6

Forbes B C, Stammler F, Kumpula T, Meschtyb N, Pajunen A and Kaarlejärvi E 2009 High resilience in the Yamal-Nenets social–ecological system, West Siberian Arctic, Russia *Proc. Natl Acad. Sci. USA* **106** 22041–8

Forbes B C, Macias-Fauria M and Zetterberg P 2010 Russian Arctic warming and 'greening' are closely tracked by tundra shrub willows *Glob. Change Biol.* **16** 1542–54

Fraser R H, Olthof I, Carrière M, Deschamps A and Pouliot D 2011 Detecting long-term changes to vegetation in northern Canada using the Landsat satellite image archive *Environ. Res. Lett.* **6** 045502

Frost G V, Epstein H E, Walker D A, Matyshak G and Ermokhina K 2013 Patterned-ground facilitates shrub expansion in Low Arctic tundra *Environ. Res. Lett.* **8** 015035

Frost G V and Epstein H E 2014 Tall shrub and tree expansion in Siberian tundra ecotones since the 1960s *Glob. Change Biol.* doi:10.1111/gcb.12406

Jia G J, Epstein H E and Walker D A 1981–2001 Greening of arctic Alaska *Geophys. Res. Lett.* **30** 2067

Leibman M O 1995 Cryogenic landslides on the Yamal Peninsula, Russia: preliminary observations *Permafrost Periglac.* **6** 259–64

Macias-Fauria M, Forbes B C, Zetterberg P and Kumpula T 2012 Eurasian Arctic greening reveals teleconnections and the potential for structurally novel ecosystems *Nature Climate Change* **2** 613–8

Masek J G, Vermote E F, Saleous N E, Wolfe R, Hall F G, Huemmrich K F, Gao F, Kutler J and Lim T-K 2006 A Landsat surface reflectance dataset for North America, 1990–2000 *IEEE Geosci. Remote Sens.* **3** 68–72

McManus K M, Morton D C, Masek J G, Wang D, Sexton J O, Nagol J R, Ropars P and Boudreau S 2012 Satellite-based evidence for shrub and graminoid tundra expansion in northern Quebec from 1986 to 2010 *Glob. Change Biol.* **18** 2313–23

Myers-Smith I H *et al* 2011 Shrub expansion in tundra ecosystems: dynamics, impacts and research priorities *Environ. Res. Lett.* **6** 045509

Myneni R B, Keeling C D, Tucker C J, Asrar G and Nemani R R 1997 Increased plant growth in the northern high latitudes from 1981 to 1991 *Nature* **386** 698–702

Peterson R A and Krantz W B 2003 A mechanism for differential frost heave and its implications for patterned-ground formation *J. Glaciol.* **49** 69–80

Raynolds M K, Walker D A, Epstein H E, Pinzon J E and Tucker C J 2012 A new estimate of tundra-biome phytomass from trans-Arctic field data and AVHRR NDVI *Remote Sens. Lett.* **3** 403–11

Raynolds M K, Walker D A, Verbyla D and Munger C A 2013 Patterns of change within a tundra landscape: 22-year Landsat NDVI trends in an area of the northern foothills of the Brooks Range, Alaska *Arct. Antarct. Alp. Res.* **45** 249–60

Serreze M C and Barry R G 2011 Processes and impacts of Arctic amplification: A research synthesis *Global Planet. Change* **77** 85–96

Shur Y, Jorgenson T, Kanevskiy M and Ping C-L 2009 *Proc. 9th Intl. Conf. on Permafrost*

Stammler F 2005 *Reindeer Nomads Meet the Market: Culture, Property and Globalisation at the End of the Land* (Muenster: Litverlag)

Tape K D, Hallinger M, Welker J M and Ruess R W 2012 Landscape heterogeneity of shrub expansion in arctic Alaska *Ecosystems* **15** 711–24

Tucker C J and Sellers P J 1986 Satellite remote sensing of primary production *Int. J. Remote Sens.* **16** 1395–416

Walker D A *et al* 2004 Frost-boil ecosystems: complex interactions between landforms, soils, vegetation and climate *Permafrost Periglac.* **15** 171–88

Walker D A *et al* 2005 The circumpolar Arctic vegetation map *J. Veg. Sci.* **16** 267–82

Walker D A *et al* 2008 Arctic patterned-ground ecosystems: a synthesis of field studies and models along a North American Arctic transect *J. Geophys. Res.* **113** G03S01

Walker D A *et al* 2009a Spatial and temporal patterns of greenness on the Yamal Peninsula, Russia: interactions of ecological and social factors affecting the Arctic normalized difference vegetation index *Environ. Res. Lett.* **4** 045004

Walker D A *et al* 2009b *Data report of the 2008 and 2008 Yamal expeditions: Nadym, Laborovaya, Vaskiny Dachi, and Kharasavey Alaska Geobotany Center* (Fairbanks, AK: Institute of Arctic Biology, University of Alaska)

Walker D A *et al* 2012 Environment, vegetation and greenness (NDVI) along the North America and Eurasia Arctic transects *Environ. Res. Lett.* **7** 015504